PHYSICAL REVIEW B VOLUME 40, NUMBER 11 15 OCTOBER 1989-I

Effect of electron-electron interaction on the thermoelectric power in disordered metallic systems

J. W. P. Hsu,* A. Kapitulnik, and M. Yu. Reizer
Department of Applied Physics, Stanford University, Stanford, California 94305

(Received 3 April 1989)

The effect of electron-electron interaction on the thermoelectric power of an impure metal is investigated. The thermoelectric coefficient η is calculated by the linear-response method as a correlation function of the electric and energy currents. It is shown that, in the three-dimensional case, the main contribution to the Seebeck coefficient $S=-\eta/\sigma$ originates from the correction to the energy-current operator due to the electron-electron interaction. In the two-dimensional case, the logarithmic temperature correction to S originates only from the corrections to the conductivity σ due to the localization and interaction effects.

I. INTRODUCTION

Recently, considerable effort has been put into studying the kinetic properties of impure and low-dimensional electronic systems.[1,2] In particular, the conductivity and the magnetoconductivity were calculated and fitted to experimental data with great success. However, the thermoelectric power (TEP) has not been as well understood. From the theoretical point of view, the difficulty in studying TEP is the fact that TEP is an odd function of the electron energy and thus is very sensitive to the structure of the electron spectrum and the electron relaxation processes.

In the presence of an electric field $\mathbf{E}$ and a temperature gradient ∇T, the electric current is

$$\mathbf{J}^e=\sigma\mathbf{E}+\eta\nabla T \tag{1}$$

where σ is the conductivity and η is the thermoelectric coefficient. In the absence of the current $\mathbf{J}^e=0$, the electric field $\mathbf{E}=S\nabla T$, where $S=-\eta/\sigma$ is the Seebeck coefficient. The condition $\mathbf{J}^e=0$ can easily be achieved experimentally by using a high-input-resistance voltmeter, thus S is normally the measured quantity. Theoretically, coefficients σ and η are calculated separately. The influence of the localization and interaction effects in TEP of a two-dimensional electron system was considered by Ting *et al.*[3] They calculated η using the linear-response method and found a logarithmic temperature correction to η similar to the well-known correction to σ.[1,2] However, it was later shown by Afonin *et al.*[4] (see also Ref. 5) that there is no logarithmic correction to η from the localization effect in the two-dimensional case.

In the present paper we consider the interaction effects on TEP in both the two- and three-dimensional cases. In particular, we show that there is no logarithmic temperature correction to η in two dimensions, contrary to Ref. 3. The logarithmic corrections to S come solely from the localization and interaction effects on the conductivity σ. The incorrect result of Ting *et al.*[3] originates from the fact that, instead of using the analytical continuation from the Matzubara frequencies, the authors performed the calculation for zero temperature and then substituted "temperature for frequency." When the analytical continuation is done correctly, the final expression for TEP depends on the combinations of $\tanh(x)$ and $d[\tanh(x)]/dx$, whose parity is important.

We further calculate the correction to the operator of the energy current from the electron-electron interaction. This correction was first studied in Ref. 6 and then discussed in Refs. 7–10 with respect to the electron-phonon interaction. The main results are obtained using the Keldysh diagram technique[11] which allows us to classify the variety of essential diagrams easily. The final results may be obtained also by using the finite-temperature Green's -function technique. The example of the analytical continuation for one of the diagrams is presented in the Appendix. The results of this calculation together with some discussion on the experimental situation are analyzed in the Summary.

II. TEP IN A SYSTEM OF INTERACTING ELECTRONS

In the Keldysh diagram technique, the electron Green's function G and the electron-electron interaction V are represented by matrices:

$$\hat{G}=\begin{bmatrix} 0 & G^A \\ G^R & G^C \end{bmatrix},\quad \hat{V}=\begin{bmatrix} 0 & V^A \\ V^R & V^C \end{bmatrix}, \tag{2}$$

where A and R denote advanced and retarded functions, respectively; G^C and V^C are defined below. The electron Green's function averaged over impurity positions equals

$$G^R(\mathbf{p},\varepsilon)=\{G^A(\mathbf{p},\varepsilon)\}^*=(\varepsilon-\xi_\mathbf{p}+i/2\tau)^{-1}, \quad \xi_\mathbf{p}=(p^2-p_F^2)/2m \tag{3}$$

where τ is the electron momentum relaxation time due to electron-impurity scattering, p_F is the Fermi momentum, m is the electron mass, and $\{\cdots\}^*$ means complex conjugate. In the linear-response method, we may take G^C to be

$$G^C(\mathbf{p},\varepsilon)=S(\varepsilon)[G^A(\mathbf{p},\varepsilon)-G^R(\mathbf{p},\varepsilon)] \tag{4}$$

where

$$S(\varepsilon)=-\tanh(\varepsilon/2T).$$

The screened electron-electron interaction for small momentum and energy transfer, $ql \ll 1$, $\omega\tau \ll 1$ (but with $p_F l \gg 1$, where $l = v_F \tau$), are[1,2]

$$V^R(\mathbf{q},\omega) = \{V^A(\mathbf{q},\omega)\}^* = 4\pi e^2 \left[q^2 + \frac{D\kappa_3^2 q^2}{-i\omega + Dq^2} \right]^{-1}, \quad d=3$$

$$= 2\pi e^2 \left[|q| + \frac{D\kappa_2 q^2}{-i\omega + Dq^2} \right]^{-1}, \quad d=2 \tag{5}$$

where d is the dimensionality of the electron system, $D = v_F^2 \tau / d$ is the diffusion constant, and κ_d is the inverse screening length ($\kappa_3^2 = 4\pi e^2 \nu_3$, $\kappa_2 = 2\pi e^2 \nu_2$), ν_d is the electron density of state summed over spins ($\nu_3 = m p_F / \pi^2$, $\nu_2 = m/\pi$), and e is the electron charge. For an electron system in equilibrium

$$V^C(\mathbf{q},\omega) = -\coth\{\omega/2T\}[V^A(\mathbf{q},\omega) - V^R(\mathbf{q},\omega)] . \tag{6}$$

In the linear-response method the thermoelectric coefficient is given by [10]

$$\eta = \frac{1}{\Omega T} \mathrm{Im}[\Pi_{xx}^R(\Omega)] , \tag{7}$$

where $\Pi^R(\Omega)$ is the Fourier representation of the retarded correlation function of the energy J_x^ε and charge J_x^e currents:

$$\Pi_{xx}^R(X - X') = -\Theta(t-t')\langle [\tilde{J}_x^\varepsilon(X), \tilde{J}_x^e(X')] \rangle , \tag{8}$$

where $\tilde{J}_x^\varepsilon(X)$ and $\tilde{J}_x^e(X')$ are operators in the Heisenberg representation, $X = (\mathbf{r}, t)$, $\mathbf{r} = (x,y,z)$, $\Theta(x)$ is the Heaviside step function, and $\langle \cdots \rangle$ represents both the thermodynamic averaging and position averaging over random impurity sites.

In the diagrammatic technique, J_x^e corresponds to the vertex Γ_x^e and J_x^ε corresponds to two verticles $\Gamma_x^{\varepsilon 0}$ and $\Gamma_x^{\varepsilon 1}$ (see Fig. 1). $\Gamma_x^{\varepsilon 1}$ contains the correction to the heat current operator due to the electron-electron interaction:[6-10]

$$\Gamma_x^e = e v_x, \quad \Gamma_x^{\varepsilon 0} = (\varepsilon + \Omega/2) v_x, \quad \Gamma_x^{\varepsilon 1} = (v_x + q_x/2m) . \tag{9}$$

The vertices of the electron-boson interaction (e.g., Γ_x^e or $\Gamma_x^{\varepsilon 0}$) in the Keldysh diagram technique acquire the factor K_{ij}^k, where the upper index is for the boson and the lower ones for electrons:

$$K_{ij}^1 = \frac{1}{\sqrt{2}} \delta_{ij}, \quad K_{ij}^2 = \frac{1}{\sqrt{2}} \begin{bmatrix} 0 & 1 \\ 1 & 0 \end{bmatrix} . \tag{10}$$

The vertex of the interaction between an electron and two bosons (e.g., $\Gamma_x^{\varepsilon 1}$) acquires a factor Q_{ij}^{kl} which equals $\frac{1}{2}$ when the number of 1's among i,j,k,l is odd, and is zero otherwise.

Within the ladder approximation (Fig. 1), the expressions for the vertex of the electron-electron interaction renormalized by impurities is as follows:

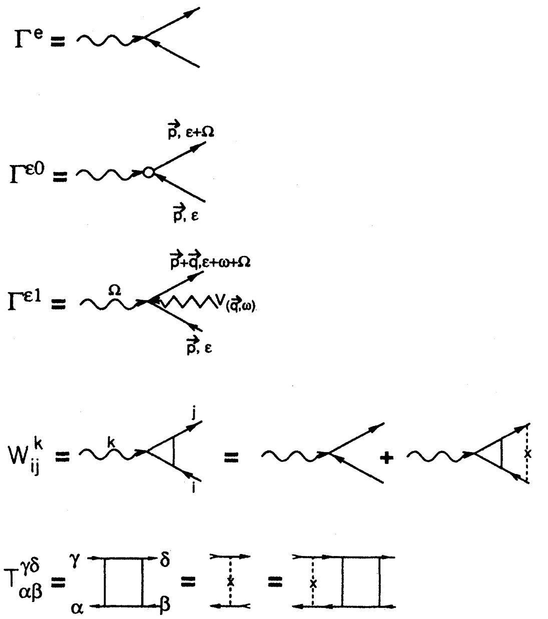

FIG. 1. Γ^e is the electric current vertex; $\Gamma^{\varepsilon 0}$ is the energy-current vertex without the electron-electron interaction; $\Gamma^{\varepsilon 1}$ is the energy-current vertex associated with the electron-electron interaction; W_{ij}^k is the scalar vertex renormalized by impurities; $T_{\alpha\beta}^{\delta\gamma}$ is the block of impurity ladders.

$$W_{22}^1 = \frac{1}{\sqrt{2}(1-\zeta)}, \quad W_{12}^1 = \frac{S(\varepsilon)\zeta}{\sqrt{2}(1-\zeta)} ,$$

$$W_{21}^1 = -\frac{S(\varepsilon+\omega)\zeta}{\sqrt{2}(1-\zeta)} ,$$

$$W_{11}^1 = \frac{1}{\sqrt{2}} \left[\frac{1}{1-\zeta^*} - 2S(\varepsilon)S(\varepsilon+\omega) \mathrm{Re} \left[\frac{\zeta}{1-\zeta} \right] \right] , \tag{11}$$

$$W_{11}^2 = -W_{21}^1 - W_{12}^1, \quad W_{22}^2 = 0, \quad W_{12}^2 = W_{21}^2 = \frac{1}{\sqrt{2}} ,$$

$$\zeta = \frac{1}{\pi \nu_d \tau} \int \frac{d^d p}{(2\pi)^d} G^A(\mathbf{p},\varepsilon) G^R(\mathbf{p},\varepsilon+\omega) = 1 + i\omega\tau - Dq^2 .$$

For the block of impurity ladders in the diffusion channel $T_{\alpha\beta}^{\gamma\delta}$ we have

$$T_{21}^{12} = T_{12}^{21} = \frac{1}{\pi\nu\tau}, \quad T_{22}^{\gamma\delta} = T_{\alpha\beta}^{22} = 0,$$

$$T_{12}^{12} = (T_{21}^{21})^* = \frac{1}{\pi\nu\tau} \frac{1}{1-\zeta} ,$$

$$T_{12}^{11} = -(T_{21}^{11})^* = \frac{-S(\varepsilon+\omega)}{\pi\nu\tau} \frac{1}{1-\zeta} , \tag{12}$$

$$T_{11}^{12} = (T_{11}^{21}) = \frac{S(\varepsilon)}{\pi\nu\tau} \frac{\zeta}{1-\zeta} ,$$

$$T_{11}^{11} = -\frac{S(\varepsilon)S(\varepsilon+\omega)}{\pi\nu\tau} 2\,\mathrm{Re} \left[\frac{\zeta}{1-\zeta} \right] .$$

The eleven diagrams essential for calculating the exchange correction to η are shown in Fig. 2. For diagrams 1, 2, 5, 10, and 11, we show only the diagrams with interaction lines on the upper Green's function. Notice the difference between the third and the fourth diagrams. For the third diagram, $\Gamma_x^{\varepsilon 0}=(\varepsilon+\Omega/2)v_x$, and for the fourth, $\Gamma_x^{\varepsilon 0}=(\varepsilon+\Omega/2+\omega/2)(v_x+q_x/2m)$. When calculating the conductivity the two vertices (Γ_x^e) are equivalent, and thus it is enough to consider only one diagram. Similarly we must consider the pairs of diagrams 6, 7 and 8, 9. For the calculation of Π^R, we need to perform a matrix product of all the elements in each diagram. This amounts to summing all contributions from each diagram with all possible ordering of the indices that are consistent with the rules described above.

Consider now the properties of the frequency-dependent functions which appear in the calculations. $S(\varepsilon)$ and $\mathrm{Im}[V^R(\omega)]$ are odd functions of their arguments, while $\partial S(\varepsilon)/\partial\varepsilon$ and $\mathrm{Re}[V^R(\omega)]$ are even. The function $f(\omega)$ defined by the following equation:

$$f(\omega)=\tfrac{1}{2}\int d\varepsilon\, S(\varepsilon+\omega)\frac{\partial S(\varepsilon)}{\partial\varepsilon}=-\tfrac{1}{2}\int d\varepsilon\, S(\varepsilon)\frac{\partial S(\varepsilon+\omega)}{\partial\varepsilon} \tag{13}$$

is odd. Thus we can write down two useful results

$$\int d\varepsilon\,\varepsilon\frac{\partial S(\varepsilon)}{\partial\varepsilon}S(\varepsilon+\omega)=\int d\varepsilon(\varepsilon+\omega)\frac{\partial S(\varepsilon+\omega)}{\partial\varepsilon}S(\varepsilon)\ , \tag{14}$$

and

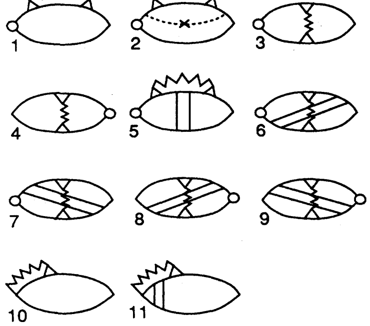

FIG. 2. Diagrams used to calculate the thermoelectric coefficient η in the linear-response method.

$$\int d\omega\int d\varepsilon\,\mathrm{Im}\{V^R(\mathbf{q},\omega)\}\varepsilon S(\varepsilon)\frac{\partial S(\varepsilon+\omega)}{\partial\varepsilon}=0\ . \tag{15}$$

For each diagram in Fig. 2, we perform first the ξ_p integration using the relations

$$\int d\xi_p G^R(G^A)^2=2\pi i\tau^2,\quad \int d\xi_p (G^R)^2(G^A)^2=4\pi\tau^3,$$
$$\int d\xi_p G^A(G^R)^3=-2\pi\tau^3\ , \tag{16}$$

which are valid under the conditions $ql \ll 1$, $\varepsilon\tau \ll 1$, and $\omega\tau \ll 1$.

For the first three diagrams, the correction to the thermoelectric coefficient is

$$\Delta\eta_{1,2,3}^d=\frac{e\tau}{T(2\pi)^2}\int d^dq\frac{1}{(2\pi)^d q^2}\int d\omega\int d\varepsilon\,\varepsilon\,\mathrm{Im}(i\omega+Dq^2)^{-1}\left[\frac{\partial}{\partial\varepsilon}[S(\varepsilon)S(\varepsilon+\omega)]-2S(\varepsilon)\frac{\partial S(\varepsilon)}{\partial\varepsilon}\right]\ . \tag{17}$$

Since $\mathrm{Im}(i\omega+Dq^2)^{-1}$ is an odd function of ω, the second term in the parentheses does not contribute. Retaining only the first term, we have

$$\Delta\eta_{1,2,3}^d=\frac{e\tau}{T(2\pi)^{2+d}}\int d^dq\frac{1}{q^2}\int_{-\infty}^{\infty}d\varepsilon\,\varepsilon\int_0^{\infty}d\omega\,\mathrm{Im}(i\omega+Dq^2)^{-1}\frac{\partial}{\partial\varepsilon}\{S(\varepsilon)[S(\varepsilon+\omega)-S(\varepsilon-\omega)]\}\ . \tag{18}$$

Defining $\varepsilon'=\varepsilon-\omega$ and shifting the argument in the second term in the parentheses in (18), we obtain

$$\Delta\eta_{1,2,3}^d=\frac{e\tau}{T(2\pi)^{2+d}}\int d^dq\frac{1}{q^2}\int_0^{\infty}d\omega\,\omega\,\mathrm{Im}(i\omega+Dq^2)^{-1}\int_{-\infty}^{\infty}d\varepsilon\frac{\partial}{\partial\varepsilon}[S(\varepsilon)S(\varepsilon+\omega)]=0\ . \tag{19}$$

Now consider the fourth diagram

$$\Delta\eta_4^d=\frac{e\tau}{T(2\pi)^{2+d}}\int d^dq\frac{1}{q^2}\int d\omega\,\mathrm{Im}(-i\omega+Dq^2)^{-1}\int d\varepsilon(\varepsilon+\omega)\left[S(\varepsilon)\frac{\partial S(\varepsilon+\omega)}{\partial\varepsilon}-S(\varepsilon+\omega)\frac{\partial S(\varepsilon)}{\partial\varepsilon}\right]\ . \tag{20}$$

Using Eqs. (13) and (14) we have

$$\Delta\eta_4^d=-\frac{2e\tau}{T(2\pi)^{2+d}}\int d^dq\frac{1}{q^2}\int d\omega\,\omega\,\mathrm{Im}(-i\omega+Dq^2)^{-1}\times f(\omega)=0\ . \tag{21}$$

Consider now the diagrams 5–9. We first note the difference between diagram 5 and diagrams 6–9. For the fifth diagram the product of the vertices is $\varepsilon v_x e v_x'$. Thus when performing the angular integration, we should expand the Green's functions from both sides of the block $T_{\alpha\beta}^{\gamma\delta}$ in power of $\mathbf{v}\cdot\mathbf{q}$ and $\mathbf{v}'\cdot\mathbf{q}$. For the diagrams 6–9 we have $\varepsilon v_x e(v_x'+q_x/m)$. If we retain the term ev_x only, we get the contribution of the same type as for the fifth diagram. We will call such contributions p terms $(\Delta\eta^q)$. The other terms, originating from eq_x/m, will be called q terms $(\Delta\eta^q)$. For the q terms, we have nonzero results of angular integration in the right part of the diagram without expansion. The q terms are not important in calculating the conductivity, but for the thermoelectric power the different analytical structures of the p and q terms results in functions which have different parity of ε and ω. Calculations show that the sum of the p terms from diagrams 5–7 is proportional to $\Delta\eta^{d}_{1,2,3}$, while the sum of the p terms from diagrams 8,9 is proportional to $\Delta\eta^{d}_{4}$.

Therefore for diagrams 1–4 and for the p terms of diagrams 5–9, a nonzero result appears only if we expand the integrands in powers of electron frequencies. The procedure of expansion is as follows. Let all electron quantities such as ν, v, and D be expanded in powers of ξ_p near the Fermi surface. Then after the ξ_p integration, all these quantities become ε dependent; τ appears from the pole of the electron Green's function $G(\mathbf{p},\varepsilon)$ and is also an ε-dependent quantity. However, it should be mentioned that we have dependence on both ε and $\varepsilon+\omega$ due to the structure of the arguments in the electron Green's functions. The same dependence on ε and $\varepsilon+\omega$ should be taken into account also in the ladder equation for W^{k}_{ij} and $T^{\gamma\delta}_{\alpha\beta}$. Nevertheless, this exact ε and $\varepsilon+\omega$ expansions only leads to very involved expressions, but cannot change the order of magnitude of the result where only the expansion in ε is considered. As we will see later, the main correction to TEP is given by diagram 11, for which we do not need the expansion. For this reason, in calculating the contribution of diagrams 1–4 and p terms of diagrams 5–9, we limit ourselves only to the ε expansion. To the same accuracy we do not distinguish diagrams 3 and 4, which differ only by ω terms in the vertices $\Gamma^{\varepsilon 0}$ in the same way as diagrams 6,7 and 8,9.

As a result, we get in the three-dimensional case

$$\Delta\eta^{3p}_{1-9}=-\frac{eT^{3/2}}{3\pi^2}\frac{\partial}{\partial\varepsilon}\left[\frac{1}{\sqrt{D}}\right]\Bigg|_{\varepsilon=\varepsilon_F}\times\left\{4\int_0^\infty\frac{dx\,x^{5/2}}{[\cosh(x)]^{1/2}}-\int_0^\infty dx\,x^{3/2}[\tanh(x)-1]\right\}. \qquad (22)$$

The first integral refers to the contribution of diagrams 5–9 and the second, in which we use the subtraction to avoid the divergence at the upper limit, refers to diagrams 1–4. The upper index p in $\Delta\eta$ means that we consider the p terms in diagrams 5–9 only. In two dimensions we have

$$\Delta\eta^{2p}_{1-9}=\frac{e}{16\pi^2 T}\int d\varepsilon\int d\omega\frac{\varepsilon}{\omega}\left\{2S(\varepsilon+\omega)\frac{\partial S(\varepsilon)}{\partial\varepsilon}-(4-\ln 2)S(\varepsilon)\times\frac{\partial S(\varepsilon+\omega)}{\partial\varepsilon}\right\}, \qquad (23)$$

where the term with the coefficient ln2 originates from diagrams 1–4. The integral in the right-hand side of (23) is zero; furthermore, there is nothing to expand in the power of ε to get a finite result, so $\Delta\eta^{2p}_{1-9}=0$.

For the q terms of diagrams 6–9 we get

$$\Delta\eta^{dq}_{6-9}=\frac{e}{(2\pi)^{d+1}Tmd^2}\int d\varepsilon\int d\omega(2\varepsilon+\omega)v^2\tau\nu_d\int d^dq\,q^2\left[S(\varepsilon+\omega)\frac{\partial S(\varepsilon)}{\partial\varepsilon}-S(\varepsilon)\frac{\partial S(\varepsilon+\omega)}{\partial\varepsilon}\right]\mathrm{Re}\left[\frac{V^R(\mathbf{q},\omega)}{(-i\omega+Dq^2)^3}\right]. \qquad (24)$$

Using Eqs. (13) and (14), we have

$$\int d\varepsilon(2\varepsilon+\omega)\left[S(\varepsilon+\omega)\frac{\partial S(\varepsilon)}{\partial\varepsilon}-S(\varepsilon)\frac{\partial S(\varepsilon+\omega)}{\partial\varepsilon}\right]=0\,. \qquad (25)$$

Doing the ε expansion in (24) and omitting ω terms in $\Gamma^{\varepsilon 0}$, we obtain the result, which is proportional to the integral

$$I=\int d\omega\int d\varepsilon\,\varepsilon^2\left[S(\varepsilon+\omega)\frac{\partial S(\varepsilon)}{\partial\varepsilon}-S(\varepsilon)\frac{\partial S(\varepsilon+\omega)}{\partial\varepsilon}\right]\phi(\omega)\,, \qquad (26)$$

where $\phi(\omega)$ is an even function. $I=0$ because the integrand is an odd function of ω, hence $\Delta\eta^{dq}_{6-9}=0$.

Now let us consider diagrams 10 and 11 which contain corrections to the energy current operator. For the p terms of diagram 10, after some transformations, we have

$$\eta^{dp}_{10}=-\frac{2e}{dT(2\pi)^{1+d}}\int d\omega f(\omega)v^2\tau\nu_d\times\int d^dq\,\mathrm{Re}\left[\frac{V^R(\mathbf{q},\omega)}{-i\omega+Dq^2}\right]=0\,. \qquad (27)$$

This is because $f(\omega)$ is an odd function of ω, but the other ω-dependent function is even. From Eq. (5) we see that

$$\frac{V^R(\mathbf{q},\omega)}{-i\omega+Dq^2}\approx\frac{1}{\nu_d Dq^2}\left[1+i\frac{\omega}{D\kappa_d^{d-1}q^{3-d}}\right]. \qquad (28)$$

It is easy to see that there are no ε-dependent terms in (27). Therefore the first-order result is also zero because there is nothing to expand. The contribution from the q terms to the tenth diagram, $\Delta\eta^{dq}_{10}$, is proportional to $\mathrm{Im}[V^R(-i\omega+Dq^2)^{-1}]$, which is very small [see (28)]; thus $\Delta\eta^{dq}_{10}$ is negligible.

For diagram 11, the contribution of the p terms in the three-dimensional case is

$$\Delta\eta_{11}^{3p}=\frac{2e}{27(2\pi)^3T}\int d\varepsilon\int d\omega\, S(\varepsilon+\omega)\frac{\partial S(\varepsilon)}{\partial\varepsilon}\times\int dq\, q^4\tau^2 v^4\nu\times\mathrm{Re}\left[\frac{V^R(\mathbf{q},\omega)}{(-i\omega+Dq^2)^2}\right]. \tag{29}$$

Without expansion of the integrand near the Fermi surface $\Delta\eta_{11}^{3p}=0$. Performing q integration we see that the combination which we need to expand is $\tau^2 v^4 D^{-5/2}$, and as a result

$$\Delta\eta_{11}^{3p}=-\frac{\sqrt{6}C}{196\pi^2}\frac{ep_F(T\tau)^{3/2}}{(\varepsilon_F\tau)^2}\approx-0.022\frac{ep_F(T\tau)^{3/2}}{(\varepsilon_F\tau)^2}\ , \tag{30}$$

where

$$C=\int dx\int dy\, x^{5/2}S(x+y)\frac{\partial S(\varepsilon)}{\partial\varepsilon}\approx 6(1-2^{-3/2})\Gamma(\tfrac{7}{2})\zeta(\tfrac{5}{2})\approx 17.3\ . \tag{31}$$

Thus $\Delta\eta_{11}^{3p}$ is of the same order as $\Delta\eta_{1-9}^{3p}$. In two dimensions, after the q integration, we have

$$\Delta\eta_{11}^{2p}=-\frac{e}{32\pi^2T}\int d\varepsilon\int d\omega\,\ln|\omega\tau|S(\varepsilon+\omega)\frac{\partial S(\varepsilon)}{\partial\varepsilon}\ . \tag{32}$$

The only ε-dependent term is $\ln|\omega\tau|$, and after the expansion

$$\Delta\eta_{11}^{2p}=-\frac{e}{16\pi^2\varepsilon_F\tau}\int d\varepsilon\,\varepsilon^2\frac{\partial S(\varepsilon)}{\partial\varepsilon}=\frac{eT}{24\varepsilon_F}\ . \tag{33}$$

For this diagram, the q-terms contribution in three dimensions equals

$$\Delta\eta_{11}^{3q}=-\frac{e}{72\pi^3mT}\times\int d\varepsilon\int d\omega\,\nu v^2\tau S(\varepsilon+\omega)\times\frac{\partial S(\varepsilon)}{\partial\varepsilon}\int dq\, q^4\times\mathrm{Im}\left[\frac{V^R(\mathbf{q},\omega)}{(-i\omega+Dq^2)^2}\right]. \tag{34}$$

Since the integrand of (34) is an even function of frequencies, a finite result is obtained without expansion near the Fermi surface:

$$\Delta\eta_{11}^{3q}=\frac{\sqrt{6}}{32\pi^2}\Gamma(\tfrac{3}{2})\zeta(\tfrac{3}{2})\frac{ep_F(T\tau)^{1/2}}{(\varepsilon_F\tau)^2}\approx 0.018\frac{ep_F(T\tau)^{1/2}}{(\varepsilon_F\tau)^2}\ . \tag{35}$$

Note that $\Delta\eta_{11}^{3q}\gg\Delta\eta_{11}^{3p}$ is due to the inequality $T\tau\ll 1$. For the two-dimensional case, after q integration, we have

$$\Delta\eta_{11}^{2q}=-\frac{e}{64\pi\varepsilon_F\tau T}\int d\omega\,\mathrm{sgn}(\omega)\int d\varepsilon\, S(\varepsilon+\omega)\frac{\partial S(\varepsilon)}{\partial\varepsilon}\ . \tag{36}$$

Neglecting the unphysical divergence at the upper limit, we find that the correction $\Delta\eta_{11}^{2q}$ is practically temperature independent:

$$\Delta\eta_{11}^{2q}=-\frac{e}{8\pi\varepsilon_F\tau}\int_0^8 dx\frac{\partial}{\partial x}[x\coth(x)]\approx\frac{e}{8\pi\varepsilon_F\tau}\ . \tag{37}$$

Now let us consider the Hartree corrections. They have the same temperature dependence as the exchange corrections but differ only by a numerical factor. We consider the Hartree corrections in the general form following Refs. 12 and 1. The electron-electron interaction is divided into two terms $V^{(j=0)}$ and $V^{(j=1)}$, where $V^{(j=0)}$ describes the interaction of an electron and a hole with the total spin $j=0$ and $V^{(j=1)}$ corresponds to $j=1$. As shown in Refs. 12 and 1

$$[V^{(j=0)}(\mathbf{q},\omega)]^R=\frac{1}{\nu_d}\frac{-i\omega+Dq^2}{Dq^2}\ , \tag{38}$$

$$[V^{(j=1)}(\mathbf{q},\omega)]^R=-\frac{F}{2\nu_d}\frac{-i\omega+Dq^2}{-i\omega(1+F/2)+Dq^2}\ , \tag{39}$$

where

$$\frac{F}{2}=-\nu_d V^{(j=1)}(\mathbf{q},\omega\to 0) \tag{40}$$

is the dimensionless interaction constant at a zero frequency. We consider only q terms of the eleventh diagram because they are the dominant contributions at low temperatures. Substituting (38) and (39) into (34) and taking into account the multiplicity of the state with $j=1$, we have

$$\Delta\eta_{11}^{3q}=\frac{\sqrt{6}}{32\pi^2}\Gamma(\tfrac{3}{2})\zeta(\tfrac{3}{2})\frac{ep_F(T\tau)^{1/2}}{(\varepsilon_F\tau)^2}\{1+3[1-(1+F/2)^{3/2}]\}, \tag{41}$$

$$\Delta\eta_{11}^{2q}=\frac{e}{8\pi\varepsilon_F\tau}\left[1-\frac{3F}{2}\right]. \tag{42}$$

In the metallic regime $F\ll 1$, the expression in the parentheses in $\Delta\eta_{11}^{3q}$ becomes $1-9F/4$.

III. SUMMARY

Because both coefficients η and σ have corrections due to the localization and interaction effects, the total expression for S is

$$S=S_0\left[1-\frac{\Delta\sigma_{\mathrm{loc}}+\Delta\sigma_{\mathrm{int}}}{\sigma_0}+\frac{\Delta\eta_{\mathrm{loc}}+\Delta\eta_{\mathrm{int}}}{\eta_0}\right], \tag{43}$$

where

$$S_0^{(d)}=-\frac{\eta_0^{(d)}}{\sigma_0^{(d)}}=\frac{\pi^2}{3e}\frac{T}{\varepsilon_F}\ . \tag{44}$$

In the three-dimensional case, $\eta_0^{(3)}=-\frac{2}{9}ep_F\tau T$ and $\sigma_0^{(d)}=e^2D\nu_d$. Thus our final result is

$$\begin{aligned}S^{(3)}=S_0^{(3)}\Bigg\{1+\frac{\sqrt{3}}{72\varepsilon_F\tau}&\left[\frac{2}{\tau}\frac{\partial}{\partial\varepsilon}\left[\frac{\tau}{\tau_\varphi}\right]^{1/2}\right|_{\varepsilon=\varepsilon_F}\\&\left.-\frac{1}{\varepsilon_F\tau}\left[\frac{\tau}{\tau_\varphi}\right]\right]\\&-(0.792+0.295-0.201)\frac{(T\tau)^{1/2}}{(\varepsilon_F\tau)^2}\\&-0.08\frac{1+3[1-(1+F/2)^{3/2}]}{(\varepsilon_F\tau)^2(T\tau)^{1/2}}\Bigg\}\,,\end{aligned}\tag{45}$$

where τ_φ is the electron phase breaking time. We used $\Delta\sigma_{\text{loc}}^{(d)}$ and $\Delta\sigma_{\text{int}}^{(d)}$ from Ref. 1, and $\Delta\eta_{\text{loc}}^{(3)}$ from Ref. 4. For $\Delta\eta_{\text{int}}^{(3)}$ we write down the contributions $\Delta\eta_{1-9}^{3p}$, $\Delta\eta_{11}^{3p}$, and $\Delta\eta_{11}^{3q}$. It is easy to see that for the condition $T\tau\ll 1$ the contribution $\Delta\eta_{11}^{3q}$ [last term in (45)] is the most important one at low temperatures. However this correction is small. For $\varepsilon_F\tau\approx 10$, we have

$$\Delta S^{(3)}=S^{(3)}-S_0^{(3)}\approx 10^{-3}(T\tau)^{-1/2}S_0^{(3)}\ .\tag{46}$$

Taking $\tau\approx 10^{-14}$ sec, $\Delta S=0.1S_0$ only at $T\approx 0.1$ K. Since S_0 for a good metal is of order of 1 μV/K, good accuracy in experimental data is required to observe this effect. Nevertheless, TEP measured on thick In-Sb films near the metal-insulator transition has been reported to observe a $T^{1/2}$ dependence for the more insulating samples.[13] The authors of Ref. 13 attributed this temperature dependence of the Seebeck coefficient to the effect of the electron-electron interaction on the conductivity. We think this $T^{1/2}$ dependence in S comes not from the interaction correction to the conductivity, but from the interaction correction to the heat-current operator in the thermoelectric coefficient.

In the two-dimensional case

$$\begin{aligned}S^{(2)}=\frac{\pi^2}{3e\varepsilon_F}\Bigg\{T+\frac{T}{2\pi\varepsilon_F\tau}&\left[\ln(\tau_\varphi/\tau)-\ln(T\tau)\left[1-\frac{3}{F}[1-2(1+F/2)\ln(1+F/2)]\right]\right]\\&-\frac{T}{2\pi\varepsilon_F\tau}\left[\frac{\partial}{\partial\varepsilon}\ln(\tau_\varphi/\tau)\Big|_{\varepsilon_F}+4\right]-\frac{3(1-3F/2)}{8\pi^2\varepsilon_F\tau^2}\Bigg\}\ .\end{aligned}\tag{47}$$

The second term in $S^{(2)}$ comes from $-\Delta\sigma^{(2)}/\sigma_0^{(2)}$, which contains the anomalous $T\ln T$ dependence. The third term originates from $\Delta\eta_{\text{loc}}^{(2)}/\eta_0^{(2)}$ and $\Delta\eta_{11}^{2q}/\eta_0^{(2)}$; this term would slightly modify the slope of the linear temperature dependence in the Seebeck coefficient. The last term in (47) is a constant and originates from $\Delta\eta_{11}^{2q}$. Since the thermoelectric power should vanish at $T=0$, this term is unphysical as T approaches 0. It originates from the perturbation approximation, which breaks down when $\Delta\eta\approx\eta_0$; this occurs for temperatures $T<T_0=3(8\pi^2\varepsilon_F\tau^2)^{-1}\approx 1$K. Nevertheless, Eq. (47) suggests that a nonzero value of S at $T=0$ can be obtained by extrapolating from the measurement of S at $T\gg T_0$. This extrapolated value will be proportional to $(\varepsilon_F\tau)^{-2}$. The result (47) is clearly different from that of Ting *et al.*, who predicted a $\ln T$ dependence in $\Delta\eta^{(2)}/\eta_0^{(2)}$. In our results, the logarithmic correction to the Seebeck coefficient comes solely from the correction to the conductivity. To date, experimental results[14–16] show a linear temperature dependence in the Seebeck coefficient for metallic samples. Thus better accuracy is needed to observe the $T\ln T$ dependence in the correction term.

ACKNOWLEDGMENTS

The authors are grateful to P. A. Lee for valuable discussion. This work was supported by the National Science Foundation under Grant No. DMR-8519753. J. W. P. Hsu acknowledges support from the Hertz Foundation.

APPENDIX

In this appendix, we shall show the calculation of diagram 11 using the finite-temperature technique. In this technique,

$$G(\mathbf{p},i\tilde{\varepsilon}_n)=(i\tilde{\varepsilon}_n-\xi_p)^{-1}\ ,$$

where

$$\tilde{\varepsilon}_n=\varepsilon_n+\frac{1}{2\tau}\operatorname{sgn}(\varepsilon_n),\quad \varepsilon_n=\pi T(2n+1)\ ,\tag{A1}$$

$$W(\mathbf{q},\varepsilon_n,\omega_m)=\frac{\Theta(\varepsilon_n)\Theta(-\varepsilon_n-\omega_m)+\Theta(-\varepsilon_n)\Theta(\varepsilon_n+\omega_m)}{\tau(|\omega_m|+Dq^2)}\,,\tag{A2}$$

$$T(\mathbf{q},\varepsilon_n,\omega_m)=\frac{1}{\pi\nu\tau}W(\mathbf{q},\varepsilon_n,\omega_m),\quad \omega_m=2\pi mT\ ,\tag{A3}$$

where $\Theta(x)$ is the Heaviside function and n,m are integers. The contribution from diagram 11 to the correlation function Π as a function of discrete frequency $\Omega_k=2\pi kT$ is

$$\begin{aligned}\Pi_{11}(\Omega_k)=-2T^2\sum_n\sum_m\int\int d\mathbf{p}\,d\mathbf{p}'\,d\mathbf{q}\frac{1}{(2\pi)^{3d}}ev_x'\frac{2p_x+q_x}{2m}&G(\mathbf{p},i\tilde{\varepsilon}_n)G(\mathbf{p}+\mathbf{q},i\tilde{\varepsilon}_n+i\tilde{\omega}_m+i\tilde{\Omega}_k)\\&\times G(\mathbf{p}'+\mathbf{q},i\tilde{\varepsilon}_n+i\tilde{\omega}_m+\tilde{\Omega}_k)G(\mathbf{p}',i\tilde{\varepsilon}_n+i\tilde{\Omega}_k)G(\mathbf{p}',i\tilde{\varepsilon}_n)V(\mathbf{q},\mathrm{i}\tilde{\omega}_\mathrm{m})\mathrm{W}(\mathbf{q},\tilde{\varepsilon}_\mathrm{n},\tilde{\omega}_\mathrm{m})\mathrm{T}(\mathbf{q},\tilde{\varepsilon}_\mathrm{n},\tilde{\omega}_\mathrm{m})\ .\end{aligned}\tag{A4}$$

We are interested in obtaining the function $\Pi^R(\Omega)$. In this case, we should consider $\Omega_k > 0$ when doing analytical continuation. The discrete sums can be transformed to the contour integrals with the formulas

$$T\sum_n \phi(i\varepsilon_n) = \frac{1}{4\pi i}\int_C d\varepsilon \tanh(\varepsilon/2T)\phi(\varepsilon) \ , \tag{A5}$$

$$T\sum_m \phi(i\omega_m) = \frac{1}{4\pi i}\int_C d\omega \coth(\omega/2T)\phi(\omega) \ , \tag{A6}$$

where C is the contour in the ε (or ω) plane along the imaginary axis in the counter clockwise direction. Taking into account the restrictions of Θ functions on $W(\mathbf{q},\varepsilon_n,\omega_m)$ and $T(\mathbf{q},\varepsilon_n,\omega_m)$, we obtain two contributions Π_{11++} when $\varepsilon_n > 0$, $\varepsilon_n + \Omega_k > 0$, $\varepsilon_n + \omega_m + \Omega_k < 0$, and Γ_{11--} when $\varepsilon_n < 0$, $\varepsilon_n + \Omega_k < 0$, $\varepsilon_n + \omega_m + \Omega_k > 0$.

Let us first consider Π_{++}. Perform the transformation from the sum over ω_m to the integral according to (A6). According to the frequency restriction mentioned above, the contour C can be changed to

$$\begin{aligned}\Pi_{11++}(\Omega_k) = -\frac{2T}{4\pi i}\sum_{\varepsilon_n}\int_{\infty - i(\varepsilon_n+\Omega_k)}^{-\infty - i(\varepsilon_n+\Omega_k)} d\omega \coth(\omega/2T)\int\int d^dp\,d^dp'\,d^dq \frac{1}{(2\pi)^{3d}} ev_x'(v_x + q_x/2m)G(\mathbf{p}, i\tilde{\varepsilon}_n)\\ \times G^A(\mathbf{p}+\mathbf{q}, \omega + i\varepsilon_n + i\Omega_k)G^A(\mathbf{p}'+\mathbf{q}, \omega + i\varepsilon_n + i\Omega_k)\\ \times G(\mathbf{p}', i\varepsilon_n + i\Omega_k)G(\mathbf{p}', i\tilde{\varepsilon}_n)\\ \times V^A(\mathbf{q},\omega)\frac{1}{\pi\nu\tau^3}\frac{1}{(i\omega + Dq^2)[i(\omega + i\Omega_k) + Dq^2]} \ .\end{aligned} \tag{A7}$$

Now let us change the variable ω to $\omega' = \omega + i\varepsilon_n + i\Omega_k$; after this transformation $\coth(\omega/2T)$ becomes $\tanh(\omega'/2T)$. We then convert the summation over ε_n to the integral over the contour C, which can be rewritten as an integral along the real axis from $-\infty$ to ∞. Now the analytical properties of all functions in the integrand are well defined and we can obtain $\Gamma_{11}^R(\Omega)$ by means of substitution $i\Omega_k \to \Omega$. Doing one more transformation $\omega \to \omega' - \varepsilon - \Omega$ we find

$$\begin{aligned}\Pi_{11++}^R(\Omega) = \frac{2}{(4\pi i)^2}\int\int d\varepsilon\, d\omega \tanh(\varepsilon/2T)\tanh\left[\frac{\varepsilon + \omega + \Omega}{2T}\right]\\ \times\int\int d^dp\,d^dp'\,d^dq\frac{1}{(2\pi)^{3d}}ev_x'\left[v_x + \frac{q_x}{2m}\right]\\ \times G^R(\mathbf{p},\varepsilon)G^A(\mathbf{p}+\mathbf{q},\omega+\varepsilon+\Omega)G^A(\mathbf{p}'+\mathbf{q},\omega+\varepsilon+\Omega)\\ \times G^R(\mathbf{p}',\varepsilon+\Omega)G^R(\mathbf{p}',\varepsilon)V^A(\mathbf{q},\omega)\frac{1}{\pi\nu\tau^3(i\omega + Dq^2)^2} \ .\end{aligned} \tag{A8}$$

Π_{11--}^R is calculated in the same manner. Contribution from diagrams with the interaction line on the lower Green's function is then added. After performing the momentum integrals, we obtain the expressions (29) and (34).

---

*Also at Department of Physics, Stanford University, Stanford, California 94305.

[1] B. L. Altshuler and A. G. Aronov, *Electron-Electron Interaction in Disordered Systems*, edited by A. L. Efros and M. Polak (North-Holland, Amsterdam, 1985).

[2] P. Lee and T. V. Ramakrishnan, Rev. Mod. Phys. **57**, 287 (1985).

[3] C. S. Ting, A. Houghton, and J. R. Senna, Phys. Rev. B **25**, 1439 (1982).

[4] V. V. Afonin, Yu. M. Galperin, and V. L. Gurevich, Zh. Eksp. Teor. Fiz. **87**, 335 (1984) [Sov. Phys—JETP **60**, 194 (1984)].

[5] C. Castellani, C. DiCastro, M. Grilli, and G. Strinati, Phys. Rev. B **37**, 6663 (1988).

[6] J. S. Langer, Phys. Rev. **128**, 110 (1962).

[7] Y. Ono, Progr. Theor. Phys. **46**, 757 (1971).

[8] S. K. Lyo, Phys. Rev. B **17**, 2545 (1978).

[9] A. Vilenkin and P. L. Taylor, Phys. Rev. B **18**, 5280 (1978).

[10] G. D. Mahan, *Many Particle Physics* (Plenum, New York 1981).

[11] L. V. Keldysh, Zh. Eksp. Teor. Fiz. **47**, 1514 (1964) [Sov. Phys.—JETP **20**, 1018 (1965)].

[12] B. L. Altshuler and A. G. Aronov, Solid State Commun. **46**, 429 (1983).

[13] A. Mawdsley, Phys Rev. B **38**, 3777 (1988).

[14] J. J. Lin, J. L. Colin, and C. Uher, *Anderson Localization*, edited by Ando and H. Fukuyama (Springer, New York, 1987), Vol. 28, p. 186.

[15] M. Burns and P. M. Chaikin, Phys. Rev. B **27**, 5924 (1983).

[16] C. Ruf, H. Obloh, B. Junge, E. Gmelin, K. Ploog, and G. Weimann, Phys. Rev. B **37**, 6377 (1988).